

S-Adapter: Generalizing Vision Transformer for Face Anti-Spoofing with Statistical Tokens

Rizhao Cai, Zitong Yu, Chenqi Kong, Haoliang Li, Changsheng Chen, Yongjian Hu, and Alex C. Kot, *Life Fellow, IEEE*

Abstract—Face Anti-Spoofing (FAS) aims to detect malicious attempts to invade a face recognition system by presenting spoofed faces. State-of-the-art FAS techniques predominantly rely on deep learning models but their cross-domain generalization capabilities are often hindered by the domain shift problem, which arises due to different distributions between training and testing data. In this study, we develop a generalized FAS method under the Efficient Parameter Transfer Learning (EPTL) paradigm, where we adapt the pre-trained Vision Transformer models for the FAS task. During training, the adapter modules are inserted into the pre-trained ViT model, and the adapters are updated while other pre-trained parameters remain fixed. We find the limitations of previous vanilla adapters in that they are based on linear layers, which lack a spoofing-aware inductive bias and thus restrict the cross-domain generalization. To address this limitation and achieve cross-domain generalized FAS, we propose a novel Statistical Adapter (S-Adapter) that gathers local discriminative and statistical information from localized token histograms. To further improve the generalization of the statistical tokens, we propose a novel Token Style Regularization (TSR), which aims to reduce domain style variance by regularizing Gram matrices extracted from tokens across different domains. Our experimental results demonstrate that our proposed S-Adapter and TSR provide significant benefits in both zero-shot and few-shot cross-domain testing, outperforming state-of-the-art methods on several benchmark tests. We will release the source code upon acceptance.

I. INTRODUCTION

Face recognition is a convenient biometric technique and people can use their faces for identity authentication. However, face recognition systems are threatened by face presentation attacks, *a.k.a.*, and face spoofing attacks. These attacks involve presenting spoofing examples of human faces to cameras, such as printed photos, digital displays, and 3D masks. Face Anti-Spoofing (FAS) [2], Face Presentation Attack Detection (Face PAD) or Face Liveness Detection, is a crucial technology that aims to enhance the security of face recognition (FR) systems by detecting malicious spoofing attacks.

Manuscript received September 2023. This work was supported by National Natural Science Foundation of China No. 62306061. Corresponding author: Zitong Yu.

Rizhao Cai, Chenqi Kong, and Alex Kot are from the ROSE Lab, School of EEE, Nanyang Technological University ({rzcai, chenqi.kong, eackot}@ntu.edu.sg).

Zitong Yu is from the School of Computing and Information Technology, Great Bay University, China (yuzitong@gbu.edu.cn).

Haoliang Li is from the Department of Electrical Engineering, City University of Hong Kong (haoliang.li@cityu.edu.hk).

Changsheng Chen is from the Shenzhen University, China (cschen@szu.edu.cn).

Yongjian Hu is with the School of Electronic and Information Engineering, South China University of Technology, Guangzhou, China, and with China-Singapore International Joint Research Institute (email: eeyjhu@scut.edu.cn).

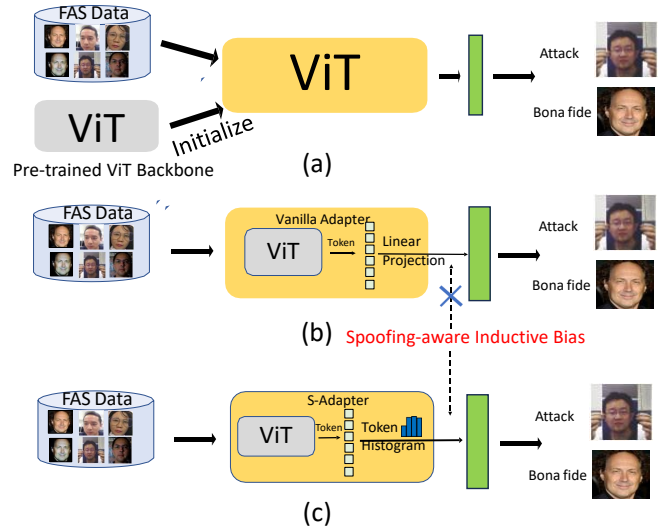


Fig. 1. (a) In the traditional transfer learning paradigm of training a ViT model for Face Anti-Spoofing task, a pre-trained Vision Transformer (ViT) model is used for initialization, which can utilize the knowledge from the pre-training dataset. Usually, the entire or a large proportion of the model parameters are fine-tuned. (b) In the cutting-edge Efficient Parameter Transfer Learning paradigm, adapter modules are integrated into a pre-trained ViT model. Throughout the training process, only the adapter module parameters are updated and the pre-trained parameters are fixed. Previous vanilla adapters, which are based on linear layers, lack the task-aware inductive bias [1], thereby limiting the utilization of pre-trained models. (c) Our proposed S-Adapter addresses this limitation by extracting localized token histograms to extract statistical information, enabling more efficient fine-tuning of the pre-trained ViT model for cross-domain generalized face anti-spoofing.

To safeguard FR systems against such malicious spoofing attacks, various techniques have been extensively researched and developed [2], [3], [4]. Traditional methods are mainly based on handcraft features and Support Vector Machines [5], [6]. Given the limited representation capability of the hand-crafted features, traditional methods cannot meet the security requirement of a FAS system. In recent years, deep neural networks have been increasingly incorporated into data-driven face anti-spoofing (FAS) methods to extract learnable features, surpassing traditional methods [2]. However, the deployment of these models is facing the domain shift problem, which arises from differences in data distribution between the source training data and the target testing data, caused by various data collection conditions, such as illumination, cameras, or attack mediums [7]. The resulting overfitting of the training distribution can lead to poor performance on the target testing data, hindering the effective detection of spoofing attacks. To

tackle the challenge in cross-domain testing, previous research has explored various techniques, including but not limited to reinforcement learning [8], adversarial learning [9], [10], meta-learning [11], [12], [13], [14], disentanglement learning [15], [16], and casual intervention [17], [18]. Despite the progress achieved, cross-domain generalization performance remains unsatisfactory due to the critical challenge posed by the domain shift problem, and further research effort is still needed.

Recently, the cutting-edge Vision Transformer (ViT) models achieve striking performance with the self-attention mechanism for computer vision tasks [19], [20]. Inspired by the success of ViT, the FAS researchers have been exploring the use of ViT to address the face anti-spoofing problem [21], [22]. While training a ViT model to the FAS task from scratch requires a large amount of data to achieve generalized performance, the model weights of ImageNet pre-trained ViT are easily available from open-source model zoos and can be used for model initialization for training a ViT model on FAS data [21], as shown in Fig. 1. However, previous works utilize the pre-trained model by fine-tuning either the partial or the whole model weights of the ViT backbone. Such utilization is straightforward but inefficient. Recent research on Efficient Parameter Transfer Learning (EPTL) has shown a more efficient way of utilizing pre-trained ViT models for the FAS problem. Huang *et al.* [22] utilized multi-stream linear adapters to adapt ViT efficiently and achieve promising generalization performance in the few-shot cross-domain scenario. However, in the zero-shot scenario, the unseen target domain testing scenario [23], the ViT's generalization performance is still inferior to the previous state-of-the-art on the four-dataset benchmark [23]. We identify the limitation of using vanilla adapters based on linear layers. Linear layers lack image-aware inductive bias, such as locality, and are thus ineffective in extracting local information [24]. Since the FAS data are visual images and the local information is crucial for the classification [8], the linear-layer-base adapter fails to capture discriminative local information to efficiently adapt ViT for FAS. Moreover, the feature/token embeddings used for FAS classification are sensitive to the imaging process, such as variations in camera modules and illuminations. Such variations between the source training and target testing data cause the domain shift and lead to models' poor domain generalization performance [7]. However, it is non-trivial to learn domain-invariant information by simply using linear layers. Nevertheless, ViT with EPTL leads to a promising direction for future research in the field of FAS and deserves further development.

Motivated by the above discussion, we propose to design a more advanced adapter, named S-Adapter for the face anti-spoofing problem, to efficiently fine-tune a pre-trained ViT for cross-domain generalized FAS. As illustrated in Fig. 2, our S-Adapter is motivated by traditional texture analysis methods, which collect histogram features from handcrafted feature maps, such as local binary pattern maps [5], [25], to alleviate the negative impact from varying environments, such as lightings. Our S-Adapter first extracts learnable discriminative token maps. Then token histograms are extracted,

which provide statistical information and improve the robustness against variations in the environment. Furthermore, the statistical information can benefit the model but its effectiveness is still hindered by the style variance between different domains. To reduce the style variance, we propose Token Style Regularization (TSR). The proposed TSR extracts style components based on the gram matrix, and regularizes the style variance of real faces from different domains to be minimized. As such, the statistical information with less style variance would be more generalized for the cross-domain FAS. We conduct extensive experiments to show that our proposed method surpasses the vanilla adapter by a clear margin and achieves state-of-the-art performance on existing cross-domain face anti-spoofing benchmarks. The contributions of our work can be summarized as follows:

- We propose a novel S-Adapter to efficiently adapt pre-trained ViT models to achieve generalized face anti-spoofing by extracting statistical information via token histograms;
- We propose a new Token Style Regularization (TSR), which reduces the style variances across different domains to improve the generalization of statistical token histograms.;
- The ViT model integrated with our proposed S-Adapter and TSR can achieve state-of-the-art generalization performance on existing face anti-spoofing benchmarks, including zero/few-shot cross-domain generalization and unseen attack detection.

II. RELATED WORKS

A. Face Anti-Spoofing.

1) *Traditional FAS Methods*: Traditional face anti-spoofing (FAS) methods rely on handcrafted image descriptors to extract features for classification, such as Local Binary Patterns (LBP) [26], [5], [25], Histogram of Gradient [6], Difference of Gaussian (DoG) [27], and image quality features [28], [29], [30]. These pioneering methods' performance is limited by the representation capability of handcraft features, and even the intra-domain performance is not satisfactory.

2) *Deep Learning FAS Methods*: Recently, numerous FAS methods based on deep neural networks have been proposed to exploit their powerful representation learning capabilities [2], [3]. For example, reinforcement learning has been proposed to mine local and global features for FAS [8]. Pixel-wise supervision has been studied to show more advanced performance than binary supervision [31], [32], [33], [34]. However, models trained solely on RGB images often suffer from overfitting and poor generalization performance when there are domain shifts between training and testing data [7]. Besides, hybrid methods, which combine handcraft features and deep learning have also been proposed [35], [36], [37], [38], [39]. While the above methods have achieved saturated performance in the intra-domain evaluation, more evaluation scenarios are raised and studied, such as domain generalization scenario [23], [12], [13], unsupervised domain adaptation scenario [15], [40], unseen attack detection scenario [41], and so on.

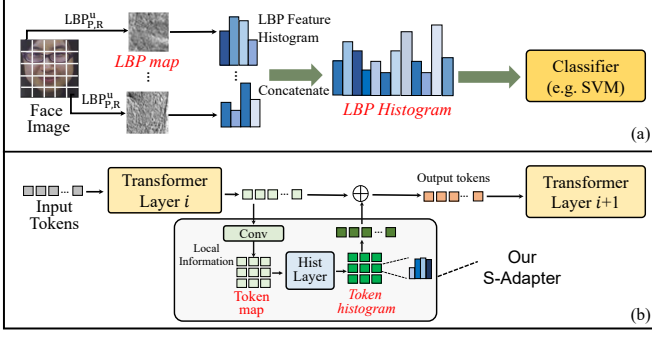


Fig. 2. (a) The process of traditional texture analysis method for face anti-spoofing: handcraft features (LBP) are first extracted, which are often sensitive to illumination changes. Then, the histogram features are extracted as final representations for the classifier, which is more robust to lighting changes. (b) Our adapter extracts local information from spatial tokens and extracts token histogram, which is inspired by (a), for improving cross-domain performance.

3) *FAS under Different Scenarios.*: The domain generalization (DG) scenario in FAS aims to learn a model with source data from one or more domains and can achieve generalized performance on unseen target data domains without using target domain data [23], [13]. Usually, the target domain data is unseen from the training, meaning the different data distributions between training and testing. This scenario is also referred to as unseen domain generalization or zero-shot cross-domain generalization. In this scenario, methods are expected to learn domain-invariant feature representations, and thus various techniques have been proposed to tackle domain generalization challenges in FAS, such as casual intervention [17], disentangled representation learning [16], [42], [43], [44], and meta-learning [14], [12], [13], [11], adversarial learning [23], [9], [10], and contrastive learning [45], [9], [46]. The domain generalization scenario is a crucial challenge since domain shift would deter a FAS model from being deployed to practical environments. Meanwhile, the unsupervised domain adaptation (UDA) for face anti-spoofing is to utilize target domain data to adapt a model pre-trained on the source domain data but without the labels of attack and bona fide examples [47], [40], [15]. Since the accessibility of labels is not often a problem, the few-shot cross-domain face anti-spoofing is studied, to utilize a few labeled target domain data (e.g. 5-shot, 10 examples) during the training to achieve great generalization performance in the target domain [48], [22]. Likewise, one-class adaptation is also studied, where only real face examples are available [49], [50], [46]. Moreover, other than common replay, print, and 3D mask attacks [51], more attack types appear such as makeup attacks, partial attacks, and obfuscation attacks. To evaluate a model's performance against unseen attack types, the unseen attack detection scenario has also been proposed and studied [52], [53], [41], [54]. In this work, we extensively evaluate our proposed method in zero-shot cross-domain (DG) and few-shot domain generalization scenarios, as well as the unseen attack detection scenario.

B. Efficient Parameter Transfer Learning for ViT

The Vision Transformer (ViT) has a key component called Multi-Head Self-Attention (MHSA). In MHSA, the input

token X is first transformed into the query (Q), key (K), and value (V): $Q = XW^Q$, $K = XW^K$, and $V = XW^V$, where W^Q , W^K , and W^V are the linear layers that transform the Q , K , and V respectively. The output with self-attention is then calculated as $\text{Softmax}(\frac{QK^T}{\sqrt{d}})V$, where d denotes the embedding dimensions of Q and K . Efficient Parameter Transfer Learning (EPTL) aims to accelerate the training process on downstream datasets by transferring knowledge from pre-trained ViT models. Typically, only a small number of parameters are updated, while the rest are initialized from the pre-trained model and kept fixed during fine-tuning.

One EPTL example is the adapter approach [55], which involves training small additional modules (adapters) on top of a pre-trained base model. The adapter contains a few task-specific layers and has been successfully applied to various computer vision tasks, such as object detection and semantic segmentation [1]. Given the input token X , the adapter \mathcal{A} usually transforms the tokens as $X \leftarrow X + \mathcal{A}(X)$.

Another EPTL example is the Low-Rank Approximation (LoRA) method [56], which approximates the weight increments of W^Q and W^K by ΔW^Q and ΔW^K . During fine-tuning, ΔW^Q and ΔW^K are approximated by extra parameters, and updated via backward propagation, while W^Q and W^K are initialized from pre-trained models and fixed. Consequently, the query $Q = XW^Q + X\Delta W^Q$ and $K = XW^K + X\Delta W^K$.

Prompt tuning [57] is another EPTL example, in which input tokens of one or more layers are concatenated with learnable prompt tokens P . This combination of pre-trained models and few-shot learning enables rapid adaptation to new tasks. In the layer with prompts, $X \leftarrow [X, P]$. The tokens X are learned from the fixed pre-trained model, while P is trainable during fine-tuning.

In this work, we focus on developing a more advanced adapter by introducing spoofing-aware inductive bias to \mathcal{A} when conducting token transformation. How to develop Prompt and LoRA for generalized FAS can be studied in the future. A prior work that is related to our work is [22], which also adopts adapters for face anti-spoofing. However, [22] only adopts simple multi-stream linear adapters for face anti-spoofing. The design of the adapters lacks insight from the data properties of the FAS task, such as locality, fine-grain information, style variances, etc. Our work incorporates the above insights in the design of our proposed S-Adapter.

III. METHODOLOGY

In this section, we first provide preliminary knowledge about how to use adapters to fine-tune the vision transformer. Subsequently, we describe how our proposed S-Adapter is developed. Finally, we describe the final optimization method, which involves the proposed Token Style Regularization in the total loss function.

A. ViT with S-Adapter

Before delving into our S-Adapter, we first provide the necessary background on Vision Transformer (ViT) and adapters.

In a ViT model [19], there can be a number of N^B feed-forward transformer blocks, where the i -th block can be represented as \mathcal{W}_i^B . As depicted in Fig. 3, each block usually contains a Multi-Head Self Attention (MHSA) layer \mathcal{W}_i^{MSA} and a Multi-Layer Perceptron (MLP) layer \mathcal{W}_i^{MLP} , and each layer is accompanied by a Layer Normalization layer and a non-linear activation layer. By simplifying the skip connections, normalization layers, and activation layers, the inference procedure of each transformer block can be expressed as:

$$Y = \mathcal{W}_i^B(X) = \mathcal{W}_i^{MLP}(\mathcal{W}_i^{MSA}(X)), \quad (1)$$

where X and Y are the input and output tokens of the block respectively.

In the traditional paradigm, ViT is pre-trained on a large-scale dataset, either by Self-Supervised Learning (SSL) or Supervised Learning (SL). Then, the pre-trained ViT is fine-tuned on a specific downstream task. Since fine-tuning the entire ViT model is challenging, recent studies on EPTL provide an efficient way of fine-tuning ViT by inserting into it small and task-specific adapter modules [1], [24]. With adapter modules, the inference process in the i -th block is turned from Eq. 1 into

$$Y = \mathcal{A}_i^{MLP}(\mathcal{W}_i^{MLP}(\mathcal{A}_i^{MSA}(\mathcal{W}_i^{MSA}(X))), \quad (2)$$

where \mathcal{A}_i^{MLP} and \mathcal{A}_i^{MSA} are the adapter modules after the MHSA and MLP layers respectively. During the fine-tuning, \mathcal{W}_i^{MLP} and \mathcal{W}_i^{MSA} are initialized by a pre-trained model, and they are fixed and not updated during the fine-tuning. On the other hand, the inserted adapter modules \mathcal{A}_i^{MSA} and \mathcal{A}_i^{MLP} are randomly initialized and updated by backward propagation.

Eq. 2 indicates the adapter's role in transforming token embeddings from the original space into a new space related to face anti-spoofing. However, vanilla adapters utilizing linear layers exhibit limitations in the embeddings transformation for a face anti-spoofing (FAS) dataset. Firstly, linear-layer adapters lack image-specific inductive biases, such as spatial locality and 2D neighborhood structure [24], which are crucial for addressing FAS challenges due to the importance of visual local features [8]. Beside, FAS classification needs more fine-grain information [58] and expects features to be robust against variations in imaging environments about illuminations and camera modules, which is non-trivial for linear layers to learn.

We propose our S-Adapter to address the above limitations to adapt pre-trained ViT for generalized face anti-spoofing efficiently. As illustrated in Fig. 2, our S-Adapter is inspired by traditional texture analysis methods in face anti-spoofing [5], [25]. In the method of using local LBP features, the LBP descriptor is first used to extract the raw LBP maps, which are at a low level and sensitive to imaging conditions [5]. Then the LBP histogram is collected, improving the feature level with histogram statistical information. The feature representation with histogram can be more robust against lighting variations, which inspires us to introduce statistical information via the proposed S-Adapter.

The design of our S-Adapter is depicted in Fig. 3, which links to the traditional LBP histogram method. The process of S-Adapter can be broken down into two main steps. The first

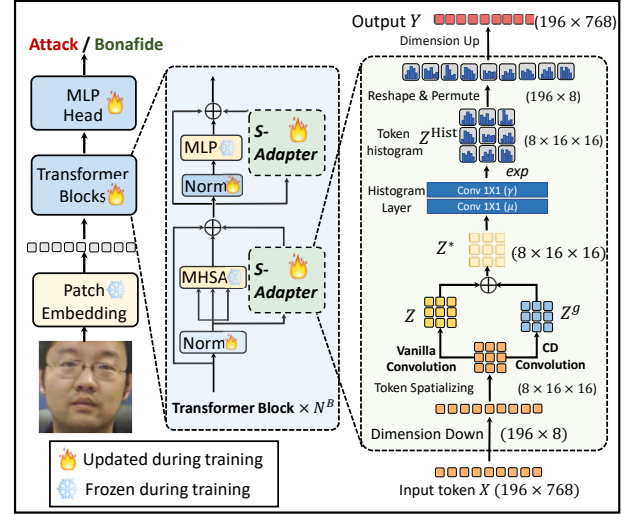


Fig. 3. The structure of ViT backbone and our S-Adapter. The S-Adapter is inserted into the ViT and updated during the training.

step is **Token Map Extraction** and this step is analogous to the extraction of raw LBP maps. The second step is **Token Histogram Extraction**, in which we collect the histograms on token maps. This step is analogous to the LBP histogram feature extraction, improving the level of token embedding more robust against environmental changes. By incorporating the S-Adapter into the ViT architecture, we enhance its capability to handle cross-domain performance while maintaining efficiency by extracting statistical information.

1) *Token Map Extraction.*: In the context of face anti-spoofing, local information is crucial for detection due to artifacts generated during the recapturing process, often appearing in local regions [8]. Since input tokens X of a transformer block are flattened without the spatial structure. To extract local information, we reconstruct the 2D structure of X . Given the input token $X \in \mathbb{R}^{N^P \times C}$, where N^P denotes the number of tokens and C represents token embedding, we first reshape X as $X^R \in \mathbb{R}^{H \times W \times C}$, with $H \times W = N^P$ (class token ignored). Then, we permute dimensions to obtain $X^M \in \mathbb{R}^{C \times H \times W}$. Consequently, tokens are represented in a 2D-image style, enabling the use of widely-used PyTorch-style 2D Convolution techniques for learning purposes.

With the spatial tokens X^M , we apply the 2D convolution \mathcal{W}^{Conv} on it to extract the token map Z in a learnable way that

$$Z = \mathcal{W}^{Conv}(X^M). \quad (3)$$

Moreover, considering that the features of spoofing artifacts are often of fine-grain details, which can be represented by the gradients based on the Center Difference (CD), we extract token gradients based on the central difference [58] of tokens. The gradient of a token Z_n can be represented as

$$Z_n^g = \sum_{p \in \mathcal{P}^n} \omega(p) \cdot (Z_p - Z_n), \quad (4)$$

where Z_n is the n -th element of Z ($n < N^P$), \mathcal{P}^n is the index sets of the spatial neighbors of tokens of Z_n , ω is the kernel

weight of \mathcal{W}^{Conv} . With the token gradients Z^g , the final token maps Z^* can be calculated as

$$Z^* = (1 - \theta)Z + \theta Z^g, \quad (5)$$

where θ is a constant ratio that balances the localized transformed tokens and the gradient of tokens.

2) *Token Histogram Extraction.*: The token map Z^* contains fine-grain texture features but remains sensitive to domain shifts. To address this issue, we propose to gather token statistics through the computation of token histograms Z^{Hist} to mitigate the domain shift problem, as statistical information can improve the representation capability [5] for the FAS task. The token histogram calculation process involves: 1) segmenting the feature range into discrete bins, and 2) enumerating the occurrences of each value within their respective bins. However, these operations are non-differentiable, which obstructs gradient calculation and prevents the model from being updated during backward propagation. To fit into the modern fashion of deep learning, we utilize the soft binning [59] and extract differentiable token histograms.

By defining the bin center and the bin width as μ and γ , respectively, given the token map $Z^* \in \mathbb{R}^{C \times H \times W}$, the soft binned histogram Z^{Hist} is defined as

$$Z_{chw}^{Hist} = \frac{1}{JK} \sum_{j=1}^J \sum_{k=1}^K e^{-\gamma_c^2 (Z_{c,h+j,w+k}^* - \mu_c)^2}, \quad (6)$$

where c denotes the channel dimension, h and w are spatial dimensions of the token histogram, J and K are the spatial sizes of the sliding window. To keep the size of tokens unchanged, $J = K = 3$, the stride of the window is 1, and the padding size is 1. Eq. 6 is differentiable and the bin center (μ) and bin width (γ) are also trainable and can be updated during the backward propagation. To learn μ and γ , Eq. 6 can be dismantled as

$$Z_{chw}^{Hist} = \frac{1}{JK} \sum_{j=1}^J \sum_{k=1}^K e^{-U_c^2}, \quad (7)$$

$$U_c = \gamma_c (Z_{c,h+j,w+k}^* - \mu_c),$$

where U_c denotes the c -th element of a vector U . U can be learned from two consecutive pixel-wise convolutional layers. In detail, we define \mathcal{W}^{Conv1} , a C -channel pixel-wise 1×1 convolution of which the kernel weight is fixed as 1 and the bias is learnable, which can serve as μ . In this way, $\mathcal{W}^{Conv1}(Z)$ leads to $Z - \mu$. Likewise, we can define \mathcal{W}^{Conv2} , a C -channel pixel-wise convolution of which the bias 0, and the learnable kernel weight can serve as γ . In this way, $\mathcal{W}^{Conv2}(X)$ leads to γX . As a result,

$$U = \mathcal{W}^{Conv2}(\mathcal{W}^{Conv1}(Z_{:,h+j,w+k}^*)), \quad (8)$$

$$U_c = \gamma_c (Z_{c,h+j,w+k}^* - \mu_c).$$

The output token histogram $Z^{Hist} \in \mathbb{R}^{C \times H \times W}$ is finally reshaped and permuted as the output token ($N^P \times 8$). Then, it is projected to $Y \in \mathbb{R}^{N^P \times 768}$ via a linear layer, which can achieve dimensional and semantic alignment for the fusion with the original tokens.

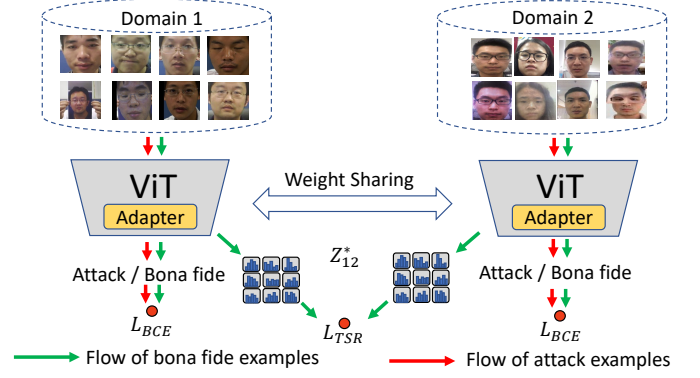


Fig. 4. The overall optimization. The bona fide and attack examples are used to calculate the binary cross-entropy loss (\mathcal{L}_{BCE}), but only the bona fide examples are used to calculate the Token Style Regularization (\mathcal{L}_{TSR}).

B. Token Style Regularization

The S-Adapter extracts statistical tokens, but the generalization of the token histogram is still affected by the variances of color and lighting, which can be summarized as style variances. To alleviate the adverse effect of learning domain-variant style components when extracting the tokens and enhance cross-domain generalization performance. Existing deep learning techniques for face anti-spoofing involve learning features from data, which can be categorized into content and style features [10]. Content features pertain to artifacts or cues crucial to the classification and are expected to be domain-invariant. By contrast, the style features encompass low-level image attributes, which are sensitive to variations in environmental changes. Diverse capturing conditions yield distinct styles, which contribute to domain shifts. Consequently, minimizing the style features learned from data is desired for domain-invariant features. Prior studies have explored disentanglement learning to separate content and style features through adversarial learning or other intricate mechanisms [16]. However, adversarial learning is often unstable, prompting us to propose TSR, a straightforward approach that does not require complex adversarial training.

Since that image style can be represented by the Gram matrix [63] of images, we formulate TSR based on the Gram matrix to minimize domain-variant styles. Given a token map $Z \in \mathbb{R}^{C \times H \times W}$, the entry (k, k') of its gram matrix can be defined as

$$G(Z)_{k,k'} = \frac{1}{CHW} \sum_{h=1}^H \sum_{w=1}^W Z_{k,h,w} Z_{k',h,w}, \quad (9)$$

where $Z_{k,h,w}$ denotes the element of Z at the coordinates of (h, w) at k -th channel. Considering that all bona fide examples can be regarded from one-domain [9], and thus their style features should be regularized to be the same. Thus, we propose our single-side Token Style Regularization, which minimizes the style variance between bona fide examples from different domains, as depicted in Fig. 4. Given tokens of bona fide examples from two domains (e.g., Z^{D1} , Z^{D2}), the TSR \mathcal{L}_{TSR} is represented as

$$\mathcal{L}_{TSR} = \|G(Z^{D1}) - G(Z^{D2})\|_F^2. \quad (10)$$

TABLE I
EXPERIMENTAL RESULTS ON THE LEAVE-ONE-OUT BENCHMARK MICO. RESULTS ARE IN TERMS OF HTER (%) AND AUC (%).

Method	Venue	C&I&O to M		O&M&I to C		O&C&M to I		I&C&M to O	
		HTER(%)	AUC(%)	HTER(%)	AUC(%)	HTER(%)	AUC(%)	HTER(%)	AUC(%)
MMD-AAE [60]	CVPR 2018	27.08	83.19	44.59	58.29	31.58	75.18	40.98	63.08
MADDG [23]	CVPR 2019	17.69	88.06	24.50	84.51	22.19	84.99	27.98	80.02
RFMetaFAS [11]	AAAI 2020	13.89	93.98	20.27	88.16	17.30	90.48	16.45	91.16
NAS-Baseline [14]	T-PAMI 2021	11.62	95.85	16.96	89.73	16.82	91.68	18.64	88.45
NAS w/ D-Meta [14]	T-PAMI 2021	16.85	90.42	15.21	92.64	11.63	96.98	13.16	94.18
NAS-FAS [14]	T-PAMI 2021	19.53	88.63	16.54	90.18	14.51	93.84	13.80	93.43
SSDG-M [9]	CVPR 2020	16.67	90.47	23.11	85.45	18.21	94.61	25.17	81.83
SSDG-R [9]	CVPR 2020	7.38	97.17	10.44	95.94	11.71	96.59	15.61	91.54
FAS-DR-BC(MT) [12]	T-PAMI 2021	11.67	93.09	18.44	89.67	11.93	94.95	16.23	91.18
SSAN-R [10]	CVPR 2022	6.57	98.78	10.00	96.67	8.88	96.79	13.72	93.62
PatchNet [61]	CVPR 2022	7.10	98.46	11.33	94.58	13.4	95.67	11.82	95.07
AMEL[62]	ACM MM 2022	10.23	96.62	11.88	94.39	18.60	88.79	11.31	93.36
MetaPattern [13]	T-IFS 2022	5.24	97.28	9.11	96.09	15.35	90.67	12.40	94.26
ViT† [22]	ECCV 2022	4.75	98.79	15.70	92.76	17.68	86.66	16.46	90.37
ViT-S-Adapter-TSR	Ours	3.43	99.50	6.32	97.82	7.16	97.61	7.21	98.00

C. Final Optimization

In the final optimization, we utilize the binary cross-entropy loss L_{BCE} , as the face anti-spoofing can be regarded as a binary classification problem, where the label “0” denotes the bonafide example and label “1” denotes spoofing attack example. When the number of domains is more than 2, we enumerate every two domains to calculate \mathcal{L}_{TSR} and then calculate the average of the \mathcal{L}_{TSR} to obtain \mathcal{L}_{TSR}^a . As such, the final loss can be represented as

$$\mathcal{L}_{total} = \mathcal{L}_{BCE} + \lambda \mathcal{L}_{TSR}^a, \quad (11)$$

where λ is a constant scaling factor. When calculating \mathcal{L}_{TSR}^a , we use the Z from the last transformer block to calculate the gram matrix.

IV. EXPERIMENT

A. Datasets, Protocols, and Implementations

Our experiments involve the use of several benchmark datasets, including CASIA-FASD [64], IDIAP REPLAY ATTACK [26], MSU MFSD [28], OULU-NPU [65], and SiW-M [53]. To evaluate our models, we employ Half-Total Error Rate (HTER), Attack Classification Error Rate (ACER), Equal Error Rate (EER), Area Under Receiver Operating Characteristic Curve (AUC), and the True Positive Rate (TPR) when False Positive Rate (FPR) equals 1% ($TPR@FPR = 1\%$). These rigorous evaluation procedures ensure the reliability and validity of our findings.

To conduct our experiments, we utilized the PyTorch 1.9 framework and performed training and testing on a single NVIDIA GTX 2080 Ti GPU. We follow [21], [22] to use ViT-Base as the ViT backbone. In data processing, we utilized MTCNN [66] to detect faces and resized the cropped face images to 224×224 as the input to the ViT-Base. During training, we employed the Adam optimizer with an initial learning rate of 0.0001.

TABLE II
EXPERIMENTAL RESULTS WITH LIMITED SOURCE DOMAINS. RESULTS ARE IN TERMS OF HTER (%) AND AUC (%).

Method	Venue	M&I to C		M&I to O	
		HTER(%)	AUC(%)	HTER(%)	AUC(%)
MS-LBP [67]	IJCB 2011	51.16	52.09	43.63	58.07
IDA [28]	T-IFS 2015	45.16	58.80	54.52	42.17
ColorTexture [5]	T-IFS 2016	55.17	46.89	53.31	45.16
LBP-TOP [68]	EJIVP 2014	45.27	54.88	47.26	50.21
MADDG [23]	CVPR 2019	41.02	64.33	39.35	65.10
SSDG-M [9]	CVPR 2020	31.89	71.29	36.01	66.88
AMEL[62]	ACM MM 2022	23.33	85.17	19.68	87.01
SSAN-M [10]	CVPR 2022	30.00	76.20	29.44	76.62
MetaPattern[13]	T-IFS 2022	30.89	72.48	20.94	86.71
ViT-S-Adapter-TSR	Ours	17.93	89.56	19.76	86.87

B. Cross-Domain Evaluation

1) *Leave-one-out cross-domain benchmark*: To begin with, we compare our proposed method with state-of-the-art methods on the leave-one-out cross-domain benchmark [23], which consists of the CASIA-FASD (C) [64], IDIAP REPLAY ATTACK (I) [26], MSU MFSD (M) [28], and OULU-NPU (O) [65] datasets. This benchmark can also be referred to as the MICO benchmark [13] and has been widely used for cross-domain performance evaluation [9], [10], [22], [14], [12], [11]. We follow the MICO benchmark’s protocols described in [23] and present our HTER and AUC results in Table I.

We conducted a fair comparison by extracting the results of ViT† from [22] without using any supplementary data from the CelebA-Spoof dataset [73]. ViT† utilizes the same ViT-Base backbone as our proposed approach. As presented in Table I, our method outperforms ViT† significantly in all four leave-one-out comparisons, indicating the effectiveness of our approach in adapting pre-trained models for domain generalization performance in unseen domains. Additionally, our approach outperforms recent state-of-the-art methods, such as SSAN-R (CVPR2022) [10] and MettaPattern (TIFS2022) [13], achieving the best results across all four leave-one-out experiments and demonstrating the cross-domain generalization performance of our method.

2) *Limited Source Domains*: Furthermore, we evaluate the performance of our proposed method when only a limited number of source domains are available. Modified from the

TABLE III

THE RESULTS OF THE 5-SHOT CROSS-DOMAIN EXPERIMENT. 5 BONA FIDE EXAMPLES AND 5 ATTACK EXAMPLES FROM THE TARGET DOMAIN ARE USED TO FINE-TUNE THE PRE-TRAINED MODEL. THE RESULTS ARE IN TERMS OF HTER (%), AUC(%) TPR(%)@FPR=1%

Method	C&I&O to M			O&M&I to C			C&M&O to I			C&I&M to O		
	HTER	AUC	TPR@FPR=1%	HTER	AUC	TPR@FPR=1%	HTER	AUC	TPR@FPR=1%	HTER	AUC	TPR@FPR=1%
ViTAF† (ECCV-2022) [22]	4.75	98.59	80.00	4.19	98.59	57.86	3.28	99.27	76.92	10.74	95.70	51.13
ViT-S-Adapter (Ours)	2.38	99.72	94.67	3.82	99.52	78.12	1.76	99.81	94.75	4.24	99.21	85.12

TABLE IV

RESULTS OF LOO PROTOCOLS ON SiW-M DATASET [53]. THE VALUES ACER(%) REPORTED ON TESTING SETS ARE OBTAINED WITH THE THRESHOLD OF 0.5. THE BEST RESULTS ARE BOLDED.

Method	Metric(%)	Replay	Print	Mask Attacks				Makeup Attacks				Partial Attacks			Average
				Half	Silicone	Trans	Paper	Manne	Obfusc	Imperson	Cosmetic	Funny Eye	Paper Glasses	Partial Paper	
Auxiliary[31]	ACER	16.8	6.9	19.3	14.9	52.1	8.0	12.8	55.8	13.7	11.7	49.0	40.5	5.3	23.6±18.5
	EER	14.0	4.3	11.6	12.4	24.6	7.8	10.0	72.3	10.1	9.4	21.4	18.6	4.0	17.0±17.7
BCN[69]	ACER	12.8	5.7	10.7	10.3	14.9	1.9	2.4	32.3	0.8	12.9	22.9	16.5	1.7	11.2±9.2
	EER	13.4	5.2	8.3	9.7	13.6	5.8	2.5	33.8	0.0	14.0	23.3	16.6	1.2	11.3±9.5
CDCN++[2]	ACER	10.8	7.3	9.1	10.3	18.8	3.5	5.6	42.1	0.8	14.0	24.0	17.6	1.9	12.7±11.2
	EER	9.2	5.6	4.2	11.1	19.3	5.9	5.0	43.5	0.0	14.0	23.3	14.3	0.0	11.9±11.8
DC-CDN[70]	ACER	12.1	9.7	14.1	7.2	14.8	4.5	1.6	40.1	0.4	11.4	20.1	16.1	2.9	11.9±10.3
	EER	10.3	8.7	11.1	7.4	12.5	5.9	0.0	39.1	0.0	12.0	18.9	13.5	1.2	10.8±10.1
SpooTrace[16]	ACER	7.8	7.3	7.1	12.9	13.9	4.3	6.7	53.2	4.6	19.5	20.7	21.0	5.6	14.2±13.2
	EER	7.6	3.8	8.4	13.8	14.5	5.3	4.4	35.4	0.0	19.3	21.0	20.8	1.6	12.0 ± 10.0
DTN[71]	ACER	9.8	6.0	15.0	18.7	36.0	4.5	7.7	48.1	11.4	14.2	19.3	19.8	8.5	16.8±11.1
	EER	10.0	2.1	14.4	18.6	26.5	5.7	9.6	50.2	10.1	13.2	19.8	20.5	8.8	16.1±12.2
DTN(MT)[12]	ACER	9.5	7.6	13.1	16.7	20.6	2.9	5.6	34.2	3.8	12.4	19.0	20.8	3.9	13.1±8.7
	EER	9.1	7.8	14.5	14.1	18.7	3.6	6.9	35.2	3.2	11.3	18.1	17.9	3.5	12.6±8.5
FAS-DR(Depth)[12]	ACER	7.8	5.9	13.4	11.7	17.4	5.4	7.4	39.0	2.3	12.6	19.6	18.4	2.4	12.6±9.5
	EER	8.0	4.9	10.8	10.2	14.3	3.9	8.6	45.8	1.0	13.3	16.1	15.6	1.2	11.8±11.0
FAS-DR(MT)[12]	ACER	6.3	4.9	9.3	7.3	12.0	3.3	3.3	39.5	0.2	10.4	21.0	18.4	1.1	10.5±10.3
	EER	7.8	4.4	11.2	5.8	11.2	2.8	2.7	38.9	0.2	10.1	20.5	18.9	1.3	10.4±10.2
ViT[72]	ACER	11.35	5.58	3.44	9.63	16.73	1.47	2.89	26.60	1.90	9.04	23.14	11.23	2.44	9.65±8.19
	EER	11.18	7.32	3.89	9.63	14.32	0.00	3.50	23.48	1.64	9.20	20.38	11.32	1.86	9.06±7.21
ViT-S-Adapter (Ours)	ACER	8.93	4.08	1.81	2.02	1.61	0.39	0.62	4.00	1.09	6.60	13.09	0.54	0.43	3.48±3.90
	EER	5.38	3.48	1.67	2.96	1.36	0.00	0.00	4.35	0.00	7.20	10.25	0.48	0.23	2.87±3.20

MICO protocol, we use data from only two source domains (“M&I”) during the training process, and present the results in Table II. In the experiments of “M&I to O”, our method performs comparably with the state-of-the-art AMEL method [62] and outperforms AMEL by a clear margin in “M&I to C”. Overall, our method can also achieve promising cross-domain performance when the number of source domain data is limited.

3) *Few-shot Cross-Domain Evaluation*: The domain generalization evaluation previously mentioned was conducted in a zero-shot cross-domain setting, wherein no target domain data was available during the training phase. In practical applications, however, it is plausible that a small amount of target domain data may be collected to adapt a model to a new target domain. Therefore, we also assessed our method in a few-shot cross-domain setting. Following [22], we performed 5-shot cross-domain experiments and displayed the results in Table III. To ensure a fair comparison, the results of “ViTAF†” [22] excluded the CelebA-Spoof dataset [73] as supplementary training data [22], which is consistent with our ViT-S-Adapter. Our S-Adapter demonstrated increased efficiency in 5-shot cross-domain testing, yielding superior results compared to the linear-layer-based adapter employed in [22]. Consequently, our S-Adapter remains promising in the few-shot cross-domain setting.

C. Unseen Attack Detection Evaluation

While the above cross-domain evaluation only involves 2D attack examples (*i.e.* print, replay), we are aware that there are more attack types appearing, such as mask attacks [53]. Therefore, it is necessary to evaluate the proposed method’s

performance in detecting various types of attacks, especially attack types unseen in the training. As such, we utilize the unseen attack evaluation protocol based on the SiW-M dataset [53]. As listed in Table IV, the SiW-M dataset includes replay attacks, print attacks, mask attacks, makeup attacks, and partial attacks. The leave-one-out unseen attack protocol in the SiW-M dataset [53] leaves one attack type as the unseen target attack type in the testing. Overall, we can see our method achieves the best ACER results in detecting unseen attack types and surpasses the state-of-the-art method by a significant margin ($> 5\%$) in terms of ACER and EER. Therefore, our S-Adapter is still effective in detecting out-of-distribution attack types.

D. Ablation Study

We conduct the ablation study to investigate the effectiveness of our proposed S-Adapter and the TSR under different λ .

1) *Effectiveness of S-Adapter*: In this study, we investigate the effectiveness of our S-Adapter in a series of cross-domain experiments without the TSR. To assess the impact of the histogram layers and token gradient, we conduct experiments under two additional configurations: 1) “S-Adapter w/o hist”, where histogram layers are removed, and 2) “S-Adapter w/o Hist($\theta = 0$)”, where both histogram layers and token gradient ($\theta = 0$) are removed. The experimental results are provided in Fig. 5. It can be seen that our S-Adapter generally outperforms the other two configurations, illustrating the advantages of extracting the token histogram. We observe that the token gradient also contributes to lower HTER values in most cases. However, in the “C&I&M to O” experiment, the inclusion

TABLE V
RESULTS OF OUR S-ADAPTER AND TSR FOR DIFFERENT ViT BACKBONES: ViT-LARGE, ViT-SMALL, AND ViT-TINY.

Backbone	Adapter	C&I&O to M		O&M&I to C		C&M&O to I		C&I&M to O	
		HTER (%)	AUC (%)	HTER (%)	AUC (%)	HTER (%)	AUC (%)	HTER (%)	AUC (%)
ViT-Tiny	S-Adapter w/o hist ($\theta = 0$)	13.04	94.17	20.68	87.90	27.08	71.43	21.28	87.13
	S-Adapter	14.95	91.89	17.75	90.68	23.46	75.94	21.38	86.91
	S-Adapter-TSR	9.92	96.00	16.00	92.22	19.41	83.67	16.24	90.91
ViT-Small	S-Adapter w/o hist ($\theta = 0$)	11.40	95.64	17.32	91.20	19.05	89.17	15.88	91.04
	S-Adapter	10.52	95.66	12.11	94.06	20.02	89.85	12.74	93.10
	S-Adapter-TSR	9.23	96.56	11.55	94.90	12.79	93.15	12.32	94.84
ViT-Large	S-Adapter w/o hist ($\theta = 0$)	11.04	95.56	8.03	97.27	13.74	86.62	11.13	94.93
	S-Adapter	4.04	99.09	7.57	96.86	10.33	96.06	11.53	95.09
	S-Adapter-TSR	2.90	99.48	7.34	97.63	8.54	97.17	8.20	97.69

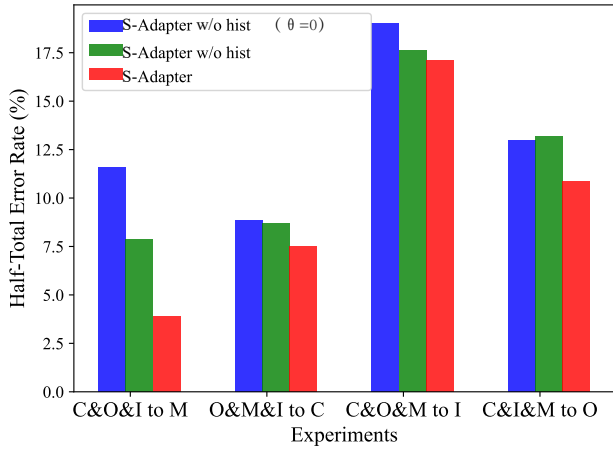


Fig. 5. Ablation study about adapters. Red bars convey the results of our S-Adapters. Green bars convey the results of removing the token histogram from our S-Adapters. Blue bars convey the results of further removing the gradient information ($\theta = 0$).

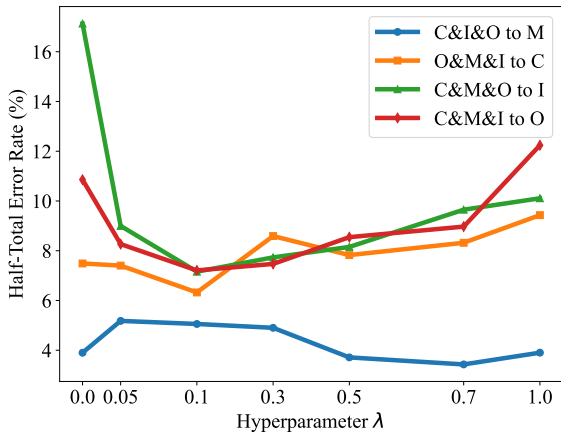


Fig. 6. The curve of HTER (%) over different λ on the leave-one-out cross-domain experiments.

of token gradient information results in an increased HTER. We conjecture that this unexpected result may be attributed to the disparity in texture between the low-resolution source domains (I, C, and M) and the high-resolution target domain

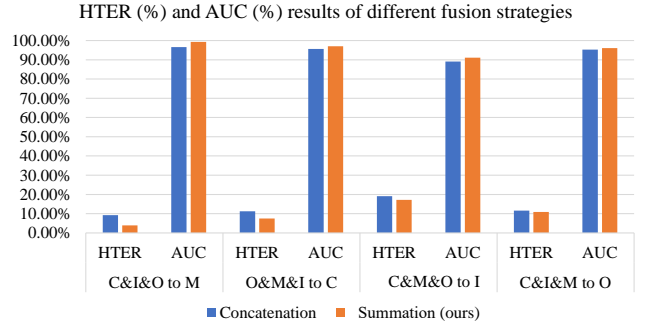


Fig. 7. Comparison between the fusion strategy of summation and concatenation. Results are in terms of HTER (%) \downarrow and AUC (%) \uparrow .

(O). Although the fine-grained texture information is extracted in the gradient, the domain gap might cause the texture to differ significantly between the low-resolution and high-resolution domains. In contrast, our histogram layers provide a more comprehensive representation of texture information across resolutions. This is evident in the lower HTER achieved by our S-Adapter compared to the other two configurations in the “C&I&M to O” experiment. In summary, our proposed S-Adapter demonstrates performance improvements by leveraging statistical information to enhance cross-domain performance, highlighting the benefits of incorporating token histogram from the token map with the gradient information.

2) *Versatility to other backbones.*: In the above experiments, we used ViT-Base to align with previous work. In this study, we examine how the proposed method can be transferred to other backbones, including ViT-tiny, ViT-Small, and ViT-Large, and the results are presented in Table V. As can be seen in Table V. The proposed S-Adapter and TSR generally benefit different backbones over the different cross-domain testing experiments. Therefore, our proposed methods are transferable.

3) *Effectiveness of TSR and λ .*: We investigate the effectiveness of our proposed TSR by altering the balancing ratio λ , and the experimental results are provided in Fig. 6. When $\lambda = 0$, TSR is not employed in the optimization process, serving as a baseline. Our proposed TSR demonstrates its ability to reduce style variance and facilitate a more generalized

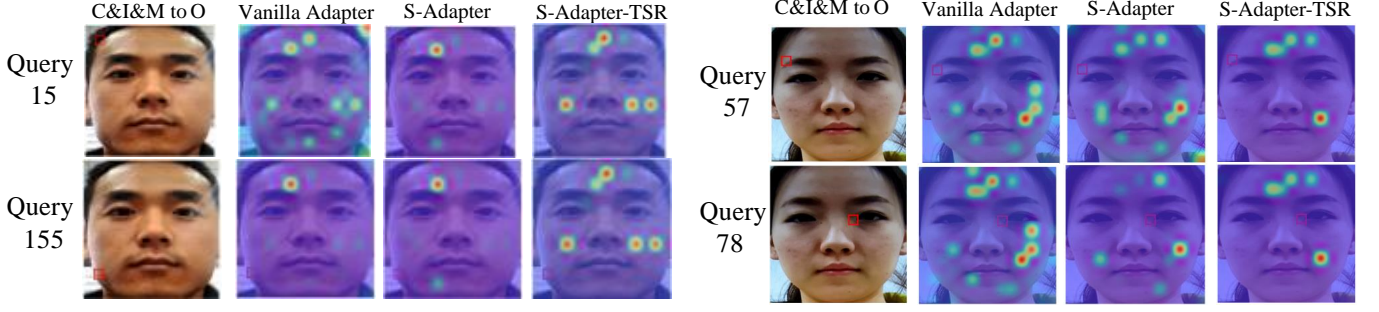


Fig. 8. Visualization of the maps of self-attention of a query patch. The left part shows an image example’s self-attention maps when the 15th (top) and 155th (bottom) are the query patch respectively. The examples are from the OULU-NPU dataset. The vanilla Adapter is based on ViT-S-Adapter but without the statistical tokens (histogram). Red means high attention and blue means low attention. Best viewed in color.

model, as evidenced by the further reduction of HTER results when a $\lambda > 0$ is applied across the four experiments. It is important to note that the optimal λ varies under different source domain settings, which is reasonable considering that different combinations of source domains possess varying style variations. However, we do not recommend using a large λ , as the model would overfit to aligning the token style and become less effective in classification. Generally, a small λ (e.g. 0.1) is advised.

4) *Study on the fusion strategy:* As depicted in Fig. 3, Y is fused with the original token input X via a summation operation. It could be argued that Y is about the statistical information, which is different from X and thus it does not make sense to do the summation between X and Y . We point out that it is Z^{Hist} that is about the statistical information, and Y has been transformed and aligned to X in terms of the semantics and dimensions via the “dimension up” (linear layer), as shown in Fig. 3. Thus, it makes sense to fuse Y with X via the summation. Nevertheless, we conduct experiments by concatenating Y to the summation result between X and the results after the MHSA. After the concatenation, the tokens’ dimension is doubled (768×2). To fix the dimension mismatch, we forward the concatenated tokens to a linear layer to reduce the dimension back to 768 to match the next layer’s input dimension. The experimental results are shown in Fig. 7. We can see that the concatenation fusion is providing poorer results. We conjecture that the extra linear layers increase the model complexity and make the model prone to overfitting.

E. Attention Map Visualization

Since the core of ViT is the self-attention mechanism, we visualize the results of self-attention from the last transformer block to analyze the model behavior. In a self-attention layer, there are N tokens of patches as input. Each output token is a weighted summation of the input tokens, where the weight matrix for each query token is calculated by self-attention. For example, in Fig. 8, the top left image shows that the 15th patch (in red rectangle) is the query, and the right sides are the attentions of the other patches, a.k.a, the weighted matrix for the summation. A patch with red attention means it contributes significantly to the output tokens of the query patch. The first row shows the attention when the 15th patch

is the query patch, and the second row shows the attention when the 155th patch is the query patch. We can see that our proposed S-Adapter and TSR can help the model to focus more consistently and intensively on the face areas (more redness). For example, we observe that our ViT-S-Adapter-TSR is consistent in the attention maps given different queries. The output attention maps of Query 15 and Query 155 are similar, meaning that the model is “keeping focus” on a similar area. On the other hand, the ViT with vanilla adapter is paying attention to various areas, since the attention maps of the two queries (15th and 155th patch) vary hugely. When the query is the 15th patch, the ViT-Adapter even focuses on the background region, instead of mining spoofing cues from the face regions. Our observations are aligned with the [74] that a vision transformer paying less attention can achieve more generalization. The observations are also consistent in the examples in the right part of Fig. 8

F. Visualization of t-SNE

We also use the t-SNE technique to visualize the distribution of class tokens (features) from the last transformer block to show the effectiveness of the proposed method. In Fig. 9, the models are trained by the combined dataset ‘C&O&M’ and the target test data is the ‘I’. Fig. 9(a) represents the t-SNE visualization of the ViT-S-Adapter without the statistical (histogram) and fine-grained information, which serves as the baseline. Fig. 9(b) represents the result of ViT-S-Adapter optimized with TSR. As can be seen in Fig. 9, the ‘real’ and ‘attack’ samples from the target (tgt) domain are overlapped and cannot be well separated (green color). By contrast, our proposed ViT-S-Adapter-TSR has better generalization capability that the ‘real’ and ‘attack’ samples from the target domains are well separated.

G. Overhead Analysis

We analyzed the overhead introduced by the S-Adapter, which contains additional parameters, by utilizing an open-source library¹ to collect data on Multiply-Accumulate operations (MACs) and the number of parameters for both the ViT (Base) model and the ViT with our S-Adapter. As illustrated

¹<https://github.com/Lyken17/pytorch-OpCounter>

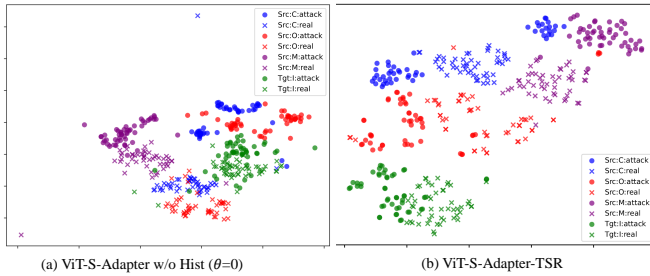


Fig. 9. The visualization of t-SNE conducted on the class token of two different adapters in the experiments of ‘C&O&M to I’. (a) is the ViT-S-Adapter without the statistical and fine-grained information ($\theta = 0$), which serves as the baseline. (b) represents our ViT-S-Adapter with the TSR.

TABLE VI

INFERENCE TIME OVERHEAD ANALYSIS. THE MACs (G) INDICATE THE TOTAL CALCULATION OPERATIONS AND THE PARAMS (M) INDICATE THE AMOUNT OF PARAMETER AND STORAGE NEEDED.

Model	MACs (G)	Params (M)
ViT	33.73	85.65
ViT-S-Adapter	33.88	85.98
Increment (Δ)	0.15 (0.45%)	0.33(0.38%)

in Table VI, the inclusion of the S-Adapter results in a modest increase of only 0.45% in MACs and a mere 0.38% in parameters overhead. Given the substantial improvement in zero/few-shot cross-domain performance and unseen attack detection capabilities provided by our S-Adapter, this minimal overhead is well justified.

V. CONCLUSION AND FUTURE WORK

In conclusion, Face Anti-Spoofing is important for the security and integrity of face recognition systems by identifying and thwarting malicious attacks. Although there has been significant progress in recent years, the domain shift problem continues to pose a challenge to a model’s cross-domain generalization performance. To tackle this issue, we introduced a novel method, S-Adapter, which effectively utilizes knowledge from pre-trained Vision Transformers (ViT) for cross-domain generalization in face anti-spoofing. Our method of S-Adapter employs the histogram information of transformer tokens and incorporates our proposed Token Style Regularization (TSR) to learn more domain-invariant feature representations. Our comprehensive experiments reveal that the proposed S-Adapter and TSR method surpasses existing techniques, achieving state-of-the-art performance on several face anti-spoofing benchmarks of zero/few-shot cross-domain evaluations, and unseen attack detection.

In the future, the proposed S-Adapter may be extended to other similar tasks such as inpainting detection, deepfake detection, and recaptured document detection problems as well. Besides, how the token histogram can be used with LoRA and Prompt can be explored in the future.

REFERENCES

- [1] Z. Chen, Y. Duan, W. Wang, J. He, T. Lu, J. Dai, and Y. Qiao, “Vision transformer adapter for dense predictions,” in *ICLR*, 2023.
- [2] Z. Yu, Y. Qin, X. Li, C. Zhao, Z. Lei, and G. Zhao, “Deep learning for face anti-spoofing: A survey,” *IEEE transactions on pattern analysis and machine intelligence*, vol. 45, no. 5, pp. 5609–5631, 2022.
- [3] C. Kong, S. Wang, and H. Li, “Digital and physical face attacks: Reviewing and one step further,” *arXiv preprint arXiv:2209.14692*, 2022.
- [4] C. Kong, K. Zheng, S. Wang, A. Rocha, and H. Li, “Beyond the pixel world: a novel acoustic-based face anti-spoofing system for smartphones,” *IEEE Transactions on Information Forensics and Security*, vol. 17, pp. 3238–3253, 2022.
- [5] Z. Boulkenafet, J. Komulainen, and A. Hadid, “Face Spoofing Detection Using Colour Texture Analysis,” *IEEE Transactions on Information Forensics and Security*, vol. 11, pp. 1818–1830, Aug 2016.
- [6] J. Komulainen, A. Hadid, and M. Pietikäinen, “Context based face anti-spoofing,” in *2013 IEEE Sixth International Conference on Biometrics: Theory, Applications and Systems (BTAS)*, pp. 1–8, 2013.
- [7] H. Li, P. He, S. Wang, A. Rocha, X. Jiang, and A. C. Kot, “Learning Generalized Deep Feature Representation for Face Anti-Spoofing,” *IEEE Transactions on Information Forensics and Security*, vol. 13, pp. 2639–2652, Oct 2018.
- [8] R. Cai, H. Li, S. Wang, C. Chen, and A. C. Kot, “DRL-FAS: A Novel Framework Based on Deep Reinforcement Learning for Face Anti-Spoofing,” *IEEE Transactions on Information Forensics and Security*, vol. 16, pp. 937–951, 2020.
- [9] Y. Jia, J. Zhang, S. Shan, and X. Chen, “Single-Side Domain Generalization for Face Anti-Spoofing,” in *2020 IEEE/CVF Conference on Computer Vision and Pattern Recognition (CVPR)*, pp. 8481–8490, 2020.
- [10] Z. Wang, Z. Wang, Z. Yu, W. Deng, J. Li, T. Gao, and Z. Wang, “Domain Generalization via Shuffled Style Assembly for Face Anti-Spoofing,” in *Proceedings of the IEEE/CVF Conference on Computer Vision and Pattern Recognition*, pp. 4123–4133, 2022.
- [11] R. Shao, X. Lan, and P. C. Yuen, “Regularized Fine-Grained Meta Face Anti-Spoofing,” *Proceedings of the AAAI Conference on Artificial Intelligence*, vol. 34, pp. 11974–11981, Apr. 2020.
- [12] Y. Qin, Z. Yu, L. Yan, Z. Wang, C. Zhao, and Z. Lei, “Meta-teacher for Face Anti-Spoofing,” *IEEE Transactions on Pattern Analysis and Machine Intelligence*, vol. Early Access, pp. 1–1, 2021.
- [13] R. Cai, Z. Li, R. Wan, H. Li, Y. Hu, and A. C. Kot, “Learning Meta Pattern for Face Anti-Spoofing,” *IEEE Transactions on Information Forensics and Security*, vol. 17, pp. 1201–1213, 2022.
- [14] Z. Yu, J. Wan, Y. Qin, X. Li, S. Z. Li, and G. Zhao, “NAS-FAS: Static-Dynamic Central Difference Network Search for Face Anti-Spoofing,” *IEEE Transactions on Pattern Analysis and Machine Intelligence*, vol. 43, no. 9, pp. 3005–3023, 2021.
- [15] G. Wang, H. Han, S. Shan, and X. Chen, “Cross-Domain Face Presentation Attack Detection via Multi-Domain Disentangled Representation Learning,” in *Proceedings of the IEEE/CVF Conference on Computer Vision and Pattern Recognition*, pp. 6678–6687, 2020.
- [16] Y. Liu, J. Stehouwer, and X. Liu, “On disentangling spoof trace for generic face anti-spoofing,” in *Computer Vision–ECCV 2020: 16th European Conference, Glasgow, UK, August 23–28, 2020, Proceedings, Part XVIII 16*, pp. 406–422, Springer, 2020.
- [17] Y. Liu, Y. Chen, W. Dai, C. Li, J. Zou, and H. Xiong, “Causal intervention for generalizable face anti-spoofing,” in *ICME*, 2022.
- [18] G. Zheng, Y. Liu, W. Dai, C. Li, J. Zou, and H. Xiong, “Learning causal representations for generalizable face anti spoofing,” in *ICASSP 2023-2023 IEEE International Conference on Acoustics, Speech and Signal Processing (ICASSP)*, pp. 1–5, IEEE, 2023.
- [19] A. Dosovitskiy, L. Beyer, A. Kolesnikov, D. Weissenborn, X. Zhai, T. Unterthiner, M. Dehghani, M. Minderer, G. Heigold, S. Gelly, et al., “An image is worth 16x16 words: Transformers for image recognition at scale,” in *International Conference on Learning Representations (ICLR)*, 2020.
- [20] Z. Liu, Y. Lin, Y. Cao, H. Hu, Y. Wei, Z. Zhang, S. Lin, and B. Guo, “Swin transformer: Hierarchical vision transformer using shifted windows,” in *Proceedings of the IEEE/CVF international conference on computer vision*, pp. 10012–10022, 2021.
- [21] A. George and S. Marcel, “On the effectiveness of vision transformers for zero-shot face anti-spoofing,” in *2021 IEEE International Joint Conference on Biometrics (IJCB)*, pp. 1–8, IEEE, 2021.
- [22] H.-P. Huang, D. Sun, Y. Liu, W.-S. Chu, T. Xiao, J. Yuan, H. Adam, and M.-H. Yang, “Adaptive transformers for robust few-shot cross-domain face anti-spoofing,” in *Computer Vision–ECCV 2022: 17th European Conference, Tel Aviv, Israel, October 23–27, 2022, Proceedings, Part XIII*, pp. 37–54, Springer, 2022.
- [23] R. Shao, X. Lan, J. Li, and P. C. Yuen, “Multi-Adversarial Discriminative Deep Domain Generalization for Face Presentation Attack Detection,”

- in *2019 IEEE/CVF Conference on Computer Vision and Pattern Recognition (CVPR)*, pp. 10015–10023, 2019.
- [24] S. Jie and Z.-H. Deng, “Convolutional bypasses are better vision transformer adapters,” *arXiv preprint arXiv:2207.07039*, 2022.
 - [25] R. Cai and C. Chen, “Learning deep forest with multi-scale local binary pattern features for face anti-spoofing,” *arXiv preprint arXiv:1910.03850*, 2019.
 - [26] I. Chingovska, A. Anjos, and S. Marcel, “On the effectiveness of local binary patterns in face anti-spoofing,” in *2012 BIOSIG - Proceedings of the International Conference of Biometrics Special Interest Group (BIOSIG)*, pp. 1–7, Sep. 2012.
 - [27] X. Tan, Y. Li, J. Liu, and L. Jiang, “Face Liveness Detection from a Single Image with Sparse Low Rank Bilinear Discriminative Model,” in *European Conference on Computer Vision*, pp. 504–517, 2010.
 - [28] D. Wen, H. Han, and A. K. Jain, “Face Spoof Detection With Image Distortion Analysis,” *IEEE Transactions on Information Forensics and Security*, vol. 10, pp. 746–761, April 2015.
 - [29] J. Galbally and S. Marcel, “Face Anti-spoofing Based on General Image Quality Assessment,” in *2014 22nd International Conference on Pattern Recognition*, pp. 1173–1178, Aug 2014.
 - [30] H. Li, S. Wang, and A. C. Kot, “Face spoofing detection with image quality regression,” in *2016 Sixth International Conference on Image Processing Theory, Tools and Applications (IPTA)*, pp. 1–6, 2016.
 - [31] Y. Liu, A. Jourabloo, and X. Liu, “Learning Deep Models for Face Anti-Spoofing: Binary or Auxiliary Supervision,” in *Proceedings of the IEEE Conference on Computer Vision and Pattern Recognition*, (Salt Lake City, UT), pp. 389–398, 2018.
 - [32] W. Sun, Y. Song, C. Chen, J. Huang, and A. C. Kot, “Face Spoofing Detection Based on Local Ternary Label Supervision in Fully Convolutional Networks,” *IEEE Transactions on Information Forensics and Security*, vol. 15, pp. 3181–3196, 2020.
 - [33] A. George and S. Marcel, “Deep Pixel-wise Binary Supervision for Face Presentation Attack Detection,” in *2019 International Conference on Biometrics (ICB)*, pp. 1–8, 2019.
 - [34] Z. Yu, X. Li, J. Shi, Z. Xia, and G. Zhao, “Revisiting Pixel-Wise Supervision for Face Anti-Spoofing,” *IEEE Transactions on Biometrics, Behavior, and Identity Science*, vol. 3, no. 3, pp. 285–295, 2021.
 - [35] L. Li, Z. Xia, A. Hadid, X. Jiang, H. Zhang, and X. Feng, “Replayed Video Attack Detection Based on Motion Blur Analysis,” *IEEE Transactions on Information Forensics and Security*, vol. 14, no. 9, pp. 2246–2261, 2019.
 - [36] M. Asim, Z. Ming, and M. Y. Javed, “CNN based spatio-temporal feature extraction for face anti-spoofing,” in *2017 2nd International Conference on Image, Vision and Computing (ICIVC)*, pp. 234–238, 2017.
 - [37] Y. A. U. Rehman, L.-M. Po, M. Liu, Z. Zou, and W. Ou, “Perturbing Convolutional Feature Maps with Histogram of Oriented Gradients for Face Liveness Detection,” in *International Joint Conference: 12th International Conference on Computational Intelligence in Security for Information Systems (CISIS 2019) and 10th International Conference on European Transnational Education (ICEUTE 2019)*, pp. 3–13, Springer, 2019.
 - [38] A. Pinto, S. Goldenstein, A. Ferreira, T. Carvalho, H. Pedrini, and A. Rocha, “Leveraging Shape, Reflectance and Albedo From Shading for Face Presentation Attack Detection,” *IEEE Transactions on Information Forensics and Security*, vol. 15, pp. 3347–3358, 2020.
 - [39] H. Chen, G. Hu, Z. Lei, Y. Chen, N. M. Robertson, and S. Z. Li, “Attention-Based Two-Stream Convolutional Networks for Face Spoofing Detection,” *IEEE Transactions on Information Forensics and Security*, vol. 15, pp. 578–593, 2020.
 - [40] Y. Liu, Y. Chen, W. Dai, M. Gou, C.-T. Huang, and H. Xiong, “Source-free domain adaptation with contrastive domain alignment and self-supervised exploration for face anti-spoofing,” in *ECCV*, 2022.
 - [41] X. Dong, H. Liu, W. Cai, P. Lv, and Z. Yu, “Open set face anti-spoofing in unseen attacks,” in *Proceedings of the 29th ACM International Conference on Multimedia*, MM ’21, (New York, NY, USA), p. 4082–4090, Association for Computing Machinery, 2021.
 - [42] K.-Y. Zhang, T. Yao, J. Zhang, Y. Tai, S. Ding, J. Li, F. Huang, H. Song, and L. Ma, “Face anti-spoofing via disentangled representation learning,” in *Computer Vision—ECCV 2020: 16th European Conference, Glasgow, UK, August 23–28, 2020, Proceedings, Part XIX 16*, pp. 641–657, Springer, 2020.
 - [43] H. Wu, D. Zeng, Y. Hu, H. Shi, and T. Mei, “Dual spoof disentanglement generation for face anti-spoofing with depth uncertainty learning,” *IEEE Transactions on Circuits and Systems for Video Technology*, 2021.
 - [44] W. Yan, Y. Zeng, and H. Hu, “Domain adversarial disentanglement network with cross-domain synthesis for generalized face anti-spoofing,” *IEEE Transactions on Circuits and Systems for Video Technology*, vol. 32, no. 10, pp. 7033–7046, 2022.
 - [45] A. Liu, C. Zhao, Z. Yu, J. Wan, A. Su, X. Liu, Z. Tan, S. Escalera, J. Xing, Y. Liang, *et al.*, “Contrastive context-aware learning for 3d high-fidelity mask face presentation attack detection,” *IEEE Transactions on Information Forensics and Security*, vol. 17, pp. 2497–2507, 2022.
 - [46] A. George and S. Marcel, “Learning one class representations for face presentation attack detection using multi-channel convolutional neural networks,” *IEEE Transactions on Information Forensics and Security*, vol. 16, pp. 361–375, 2020.
 - [47] H. Li, W. Li, H. Cao, S. Wang, F. Huang, and A. C. Kot, “Unsupervised Domain Adaptation for Face Anti-Spoofing,” *IEEE Transactions on Information Forensics and Security*, vol. 13, pp. 1794–1809, July 2018.
 - [48] Y. Qin, C. Zhao, X. Zhu, Z. Wang, Z. Yu, T. Fu, F. Zhou, J. Shi, and Z. Lei, “Learning meta model for zero-and few-shot face anti-spoofing,” in *Proceedings of the AAAI Conference on Artificial Intelligence*, vol. 34, pp. 11916–11923, 2020.
 - [49] Z. Li, R. Cai, H. Li, K.-Y. Lam, Y. Hu, and A. C. Kot, “One-class knowledge distillation for face presentation attack detection,” *IEEE Transactions on Information Forensics and Security*, vol. 17, pp. 2137–2150, 2022.
 - [50] Y. Qin, W. Zhang, J. Shi, Z. Wang, and L. Yan, “One-class adaptation face anti-spoofing with loss function search,” *Neuro Computing*, vol. 417, pp. 384–395, 2020.
 - [51] S. Jia, X. Li, C. Hu, G. Guo, and Z. Xu, “3d face anti-spoofing with factorized bilinear coding,” *IEEE Transactions on Circuits and Systems for Video Technology*, vol. 31, no. 10, pp. 4031–4045, 2020.
 - [52] Z. Li, H. Li, K.-Y. Lam, and A. C. Kot, “Unseen Face Presentation Attack Detection with Hypersphere Loss,” in *ICASSP 2020 - 2020 IEEE International Conference on Acoustics, Speech and Signal Processing (ICASSP)*, pp. 2852–2856, 2020.
 - [53] B. Liu, Z. Wu, H. Hu, and S. Lin, “Deep metric transfer for label propagation with limited annotated data,” in *ICCV Workshop*, pp. 0–0, 2019.
 - [54] A. George, Z. Mostaani, D. Geissenbuhler, O. Nikisins, A. Anjos, and S. Marcel, “Biometric face presentation attack detection with multi-channel convolutional neural network,” *IEEE Transactions on Information Forensics and Security*, vol. 15, pp. 42–55, 2020.
 - [55] N. Houlsby, A. Giurugu, S. Jastrzebski, B. Morrone, Q. De Laroussilhe, A. Gesmundo, M. Attariyan, and S. Gelly, “Parameter-efficient transfer learning for nlp,” in *International Conference on Machine Learning*, pp. 2790–2799, PMLR, 2019.
 - [56] E. J. Hu, Y. Shen, P. Wallis, Z. Allen-Zhu, Y. Li, S. Wang, L. Wang, and W. Chen, “Lora: Low-rank adaptation of large language models,” *arXiv preprint arXiv:2106.09685*, 2021.
 - [57] M. Jia, L. Tang, B.-C. Chen, C. Cardie, S. Belongie, B. Hariharan, and S.-N. Lim, “Visual prompt tuning,” in *Computer Vision—ECCV 2022: 17th European Conference, Tel Aviv, Israel, October 23–27, 2022, Proceedings, Part XXXIII*, pp. 709–727, Springer, 2022.
 - [58] Z. Yu, C. Zhao, Z. Wang, Y. Qin, Z. Su, X. Li, F. Zhou, and G. Zhao, “Searching Central Difference Convolutional Networks for Face Anti-Spoofing,” in *2020 IEEE/CVF Conference on Computer Vision and Pattern Recognition (CVPR)*, pp. 5294–5304, 2020.
 - [59] J. Peebles, W. Xu, and A. Zare, “Histogram layers for texture analysis,” *IEEE Transactions on Artificial Intelligence*, vol. 3, no. 4, pp. 541–552, 2022.
 - [60] H. Li, S. J. Pan, S. Wang, and A. C. Kot, “Domain Generalization with Adversarial Feature Learning,” in *Proceedings of the IEEE Conference on Computer Vision and Pattern Recognition*, pp. 5400–5409, 2018.
 - [61] C.-Y. Wang, Y.-D. Lu, S.-T. Yang, and S.-H. Lai, “PatchNet: A Simple Face Anti-Spoofing Framework via Fine-Grained Patch Recognition,” in *Proceedings of the IEEE/CVF Conference on Computer Vision and Pattern Recognition*, pp. 20281–20290, 2022.
 - [62] Q. Zhou, K.-Y. Zhang, T. Yao, R. Yi, S. Ding, and L. Ma, “Adaptive mixture of experts learning for generalizable face anti-spoofing,” in *Proceedings of the 30th ACM International Conference on Multimedia*, pp. 6009–6018, 2022.
 - [63] J. Johnson, A. Alahi, and L. Fei-Fei, “Perceptual losses for real-time style transfer and super-resolution,” in *Computer Vision—ECCV 2016: 14th European Conference, Amsterdam, The Netherlands, October 11–14, 2016, Proceedings, Part II 14*, pp. 694–711, Springer, 2016.
 - [64] Z. Zhang, J. Yan, S. Liu, Z. Lei, D. Yi, and S. Z. Li, “A face anti-spoofing database with diverse attacks,” in *IAPR International Conference on Biometrics*, pp. 26–31, 2012.
 - [65] Z. Boulkenafet, J. Komulainen, L. Li, X. Feng, and A. Hadid, “OULU-NPU: A mobile face presentation attack database with real-world

- variations,” in *IEEE International Conference on Automatic Face and Gesture Recognition*, May 2017.
- [66] K. Zhang, Z. Zhang, Z. Li, and Y. Qiao, “Joint Face Detection and Alignment Using Multitask Cascaded Convolutional Networks,” *IEEE Signal Processing Letters*, vol. 23, no. 10, pp. 1499–1503, 2016.
 - [67] J. Määttä, A. Hadid, and M. Pietikäinen, “Face spoofing detection from single images using micro-texture analysis,” in *2011 International Joint Conference on Biometrics (IJCB)*, pp. 1–7, 2011.
 - [68] T. de Freitas Pereira, J. Komulainen, A. Anjos, J. M. De Martino, A. Hadid, M. Pietikäinen, and S. Marcel, “Face liveness detection using dynamic texture,” *EURASIP Journal on Image and Video Processing*, vol. 2014, no. 1, p. 2, 2014.
 - [69] Z. Yu, X. Li, X. Niu, J. Shi, and G. Zhao, “Face anti-spoofing with human material perception,” in *Computer Vision—ECCV 2020: 16th European Conference, Glasgow, UK, August 23–28, 2020, Proceedings, Part VII 16*, pp. 557–575, Springer, 2020.
 - [70] Z. Yu, Y. Qin, H. Zhao, X. Li, and G. Zhao, “Dual-Cross Central Difference Network for Face Anti-Spoofing,” in *2021 International Joint Conference on Artificial Intelligence (IJCAI)*, 2021.
 - [71] Y. Liu, J. Stehouwer, A. Jourabloo, and X. Liu, “Deep Tree Learning for Zero-Shot Face Anti-Spoofing,” in *2019 IEEE/CVF Conference on Computer Vision and Pattern Recognition (CVPR)*, pp. 4675–4684, 2019.
 - [72] C.-H. Liao, W.-C. Chen, H.-T. Liu, Y.-R. Yeh, M.-C. Hu, and C.-S. Chen, “Domain invariant vision transformer learning for face anti-spoofing,” in *Proceedings of the IEEE/CVF Winter Conference on Applications of Computer Vision*, pp. 6098–6107, 2023.
 - [73] Y. Zhang, Z. Yin, Y. Li, G. Yin, J. Yan, J. Shao, and Z. Liu, “Celeba-spoof: Large-scale face anti-spoofing dataset with rich annotations,” in *European Conference on Computer Vision (ECCV)*, 2020.
 - [74] Z. Pan, B. Zhuang, H. He, J. Liu, and J. Cai, “Less is more: Pay less attention in vision transformers,” in *Proceedings of the AAAI Conference on Artificial Intelligence*, vol. 36, pp. 2035–2043, 2022.